Available online at www.sciencedirect.com
SCIENCE DIRECT®
Journal of Chromatography A, 1043 (2004) 135–147
JOURNAL OF CHROMATOGRAPHY A
www.elsevier.com/locate/chroma

Modeling continuous aqueous two-phase systems for control purposes

Laurent Simon*, Shalini Gautam

Otto H. York Department of Chemical Engineering, New Jersey Institute of Technology, University Heights, 323 Dr. Martin Luther King, Jr., Newark, NJ 07102, USA

Received 4 June 2003; received in revised form 25 September 2003; accepted 28 May 2004

Abstract

A mathematical model was proposed to allow the analysis of steady-state and transient behaviors of single-stage continuous aqueous two-phase systems. Since the complete system of simultaneous equations contains more equations than unknown variables, a program based on the method of least squares was developed to solve the problem. The methodology was tested using a system composed of thaumatin, sodium chloride, and a contaminant protein. A poly(ethylene-glycol)/phosphate salt/water system was selected to isolate the thaumatin. For the steady-state and transient operations, a constrained optimization procedure - from the Matlab Optimization Toolbox (MathWork, Inc.)—was implemented after recasting the system of equations as a minimization problem. Euler's method was used in the transient case to discretize the differential equations. The steady-state concentrations agreed with published data. An input–output model based on a 4% step change decrease in the inlet stream flow rate showed that output variables such as concentrations of sodium chloride and phosphate salt settled to their final values in different time periods. The proposed analysis may be helpful in the dynamic control of large-scale commercial extractor units using advanced control schemes.

Keywords: Aqueous two-phase systems; Degree of freedom; Mathematical modeling

1. Introduction

Aqueous two-phase systems (ATPS) have been used extensively in pharmaceutical research for the separation and purification of biomolecules. Two viscous, immiscible liquid phases are formed when two polymers (i.e. PEG/Dextran), or a polymer and a salt (i.e. PEG/Phosphate salt) are dissolved in water. The main advantages of these types of extraction processes are their biocompatibility, ease of scale-up, and low operation costs [1,2]. Furthermore, these methods are approved by regulatory agencies [3]. Compared to current separation methods, ATPS are versatile and can be designed for enzyme extraction and purification based on size, molecular mass, conformation, charge and/or hydrophobicity [1].

To make ATPS economically viable and further reduce potential impact on wastewater, polymer/polymer systems have been replaced by polymer/salt systems in most large-scale applications. This shift is partly due to the high cost of Dextran, commonly used as the bottom phase. The low viscosity and short phase separation time, is also an asset of polymer/salt systems [4]. The upper phase is usually rich in PEG, which is biodegradable and non-toxic. The bottom phase is rich in salt, namely sulfate, phosphate, or citrate. The product, with more affinity to one of the phases, is recovered in that phase while the waste containing cell debris is directed to the other phase. Recycling of the final PEG-rich phase helps to minimize PEG loss.

In large-scale separations, the two phases are equilibrated and separated either by gravity (mixer–settler) or by disk stack centrifuges. Some of the advantages of continuous crosscurrent extraction over batch processing are a shorter residence time, the use of extreme pH conditions and relatively high temperatures with negligible loss of protein activity. Because of the number of variables, such as pH and temperature, that can be manipulated to direct the partitioning of target molecules, control of continuous aqueous two-phase extraction is attractive from an industrial viewpoint. However, as in most chemical processes, the

* Corresponding author. Tel.: +1-973-536-5263; fax: +1-973-596-8436.
E-mail address: laurent.simon@njit.edu (L. Simon).

0021-9673/$ – see front matter © 2004 Elsevier B.V. All rights reserved.
doi:10.1016/j.chroma.2004.05.092

development of a mathematical model is a prerequisite for designing an adequate controller. Using an experimental approach to tune controllers for ATPS can be time consuming and quite costly. These techniques would involve testing different flow rate profiles and monitoring the protein concentrations in the system. Also, in cases where a control design step precedes the construction of the plant, a theoretical approach becomes a necessary tool. As outlined by Petrides et. al., one of the advantages of process simulation is that the impact of process changes can be assessed immediately and documented in a systematic manner [5].

Two-phase systems have been investigated extensively to describe the mechanism responsible for phase separation [1,6]. These theoretical studies help in understanding the factors influencing protein partitioning. The derived models provide invaluable tools for scale-up purposes and further system optimization. Knowing, for instance, that protein extraction in ATPS is influenced by temperature, can help the process engineer to design a temperature-induced separation process, in which heat is added or removed in order to improve product yield. However, process scale-up offers unique challenges, such as meeting production requirements in the presence of disturbances and decreasing downtime, that are not addressed in current modeling frameworks. The dynamic behavior of these systems has to be investigated and understood to enhance plant-wide control of continuous ATPS and assess safety and environmental risks at the earliest possible design stage [7].

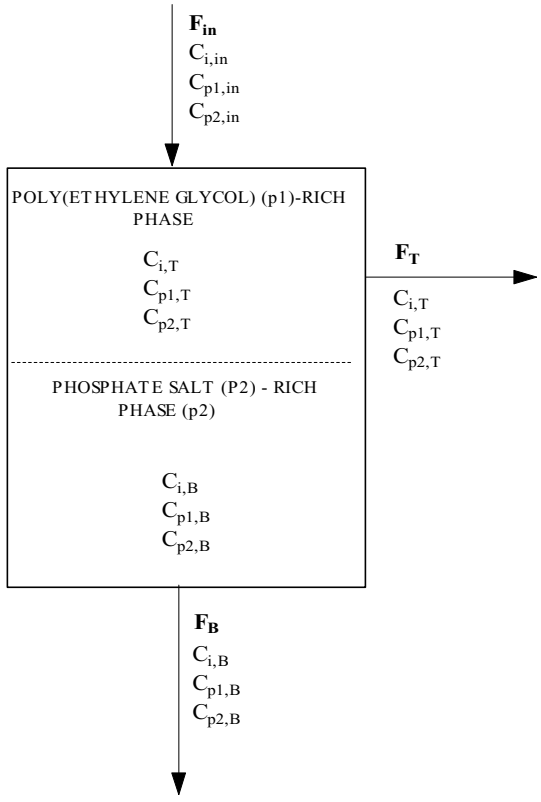

Fig. 1. Flow scheme of the single aqueous two-phase continuous protein extraction. F_{in}, F_T, and F_B are the inlet, process and waste streams, respectively.

2. Mathematical modeling of single-stage continuous ATPS

The basic components of the aqueous two-phase system, used in this study, are a polymer (p_1), a salt (or another polymer) (p_2), and water (Fig. 1). The system is composed of at least 4 components: water, polymer (p_1), polymer or salt (p_2), and a biomolecule (i). The top phase is rich in polymer p_1 (i.e., PEG), and the bottom is rich in p_2 (i.e., Dextran or phosphate salt).

Assuming quasi steady-state approximation, the total continuity equation is:

$$\frac{\mathrm{d}\,(\rho_T V_T + \rho_B V_B)}{\mathrm{d}t} = F_{in}\rho_{in} - F_T\rho_T - F_B\rho_B \quad (1)$$

where F_T and F_B are the volumetric flow rates of the output stream from the top and bottom phase, respectively. The feed F_{in} is a heterogeneous two-phase stream containing the various components. The global composition of that stream is located above the binodal curve. In order to simplify Eq. (1), we make the following assumption: the effect of compositions and temperatures on the densities is neglected, and the densities of the heterogeneous mixture (ρ_{in}), the top (ρ_T) and bottom phase (ρ_B) are approximately equal: $\rho_B \approx \rho_T \approx \rho_{in}$. A deviation from this assumption may introduce error in the simulation and will be addressed in a later section. In practice, the two phases are separated in the equipment by gravity in accordance with the phase equilibrium concentrations given by the tie-lines. This separation requires a density difference between the top and bottom phases ($\rho_B > \rho_T$) such that $\rho_B > \rho_{in} > \rho_T$ For PEG-salt systems, for instance, this difference may be in the range of 40–100 kg/m^3. In this work, we assume that $\rho_B \approx \rho_T$ (therefore $\rho_B \approx \rho_T \approx \rho_{in}$) and use Eq. (1) to write:

$$\frac{\mathrm{d}(V_T + V_B)}{\mathrm{d}t} = F_{in} - F_T - F_B \quad (2)$$

Mistry et. al. [8] used a similar assumption when performing steady-state mass balances for the main units in a two-stage PEG4000/Phosphate system to extract thaumatin. Although it was not specifically stated, they have assumed that no significant density variation exists within the system when the inlet and exit volumetric flow rates were set to be equal. Within the scope of the analysis presented in this paper, it is sufficient to mention that the difference in phase densities is not significant to the point of influencing the computed final compositions of the components in the system. However, this difference is large enough to drive the phase separation in the equipment by gravity.

The species balances are:

$$\frac{\mathrm{d}(V_T C_{i,T} + V_B C_{i,B})}{\mathrm{d}t} = F_{in}C_{i,in} - F_T C_{i,T} - F_B C_{i,B} \quad (3)$$

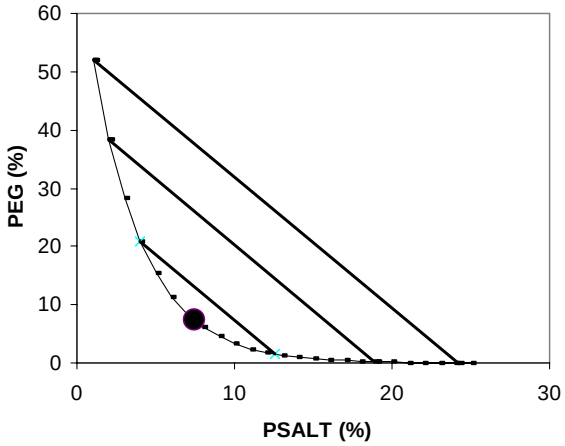

Fig. 2. Typical phase diagram of a mixture of PEG (p1), phosphate salt (p2) and water.

$$\frac{\mathrm{d}(V_{\mathrm{T}}C_{\mathrm{p1,T}} + V_{\mathrm{B}}C_{\mathrm{p1,B}})}{\mathrm{d}t} = F_{\mathrm{in}}C_{\mathrm{p1,in}} - F_{\mathrm{T}}C_{\mathrm{p1,T}} - F_{\mathrm{B}}C_{\mathrm{p1,B}} \tag{4}$$

$$\frac{\mathrm{d}(V_{\mathrm{T}}C_{\mathrm{p2,T}} + V_{\mathrm{B}}C_{\mathrm{p2,B}})}{\mathrm{d}t} = F_{\mathrm{in}}C_{\mathrm{p2,in}} - F_{\mathrm{T}}C_{\mathrm{p2,T}} - F_{B}C_{\mathrm{p2,B}} \tag{5}$$

The variable $C_{x,y}$, represents the concentration of component x in stream y. The process variables and parameters are defined in the Nomenclature. The partition coefficient of component i (K_i) is assumed to be constant:

$$K_i = \frac{C_{i,\mathrm{T}}}{C_{i,\mathrm{B}}} \tag{6}$$

In practice, the partition coefficient is a function of the system compositions, temperature and pH (i.e., concentrations of potassium hydrogen phosphate and potassium dihydrogen phosphate). For this study, we assume that the perturbations in the system concentrations are relatively small and that the system is always operating near the same tie-line region in the phase diagram. As a result, the influences of the concentration disturbances on the partition coefficients are negligible and do not affect the final composition of the system.

The phase behaviors at equilibrium are defined by the binodal curve (Fig. 2), which divides a two-phase region (above the curve) from a single-phase region (below the curve):

$$C_{\mathrm{p1,T}} = f_{\mathrm{a}}(C_{\mathrm{p2,T}}) \tag{7}$$

$$C_{\mathrm{p1,B}} = f_{\mathrm{a}}(C_{\mathrm{p2,B}}) \tag{8}$$

Mistry et al. [8] used an exponential function to represent f_{a} because it described, fairly well, phase equilibrium data for a PEG4000/Phosphate system used in prior studies [1]. The simplified model was sufficient to explain the binodal curve. However, in theory, phase diagrams are obtained by analysis of the basic thermodynamic properties of the system [9]. In general, a system, with a known total composition, separates, by centrifugation, into an upper and a lower phase, connected by a tie line. The compositions of both phases in equilibrium are calculated using expressions for the chemical potentials of all species in solution, activity coefficient models, and interaction parameters obtained by fitting the model equations to the tie-line experimental values. Since the tie-line connects equilibrium concentrations of both phases, the binodal is obtained by joining points located at the extremities of a few tie-lines generated using the above method.

The slope M of the tie-lines is given by:

$$M = \frac{C_{\mathrm{p1,T}} - C_{\mathrm{p1,B}}}{C_{\mathrm{p2,T}} - C_{\mathrm{p2,B}}} \tag{9}$$

Although the assumption of strictly parallel tie-lines is solely based on empirical observations (in fact, no analytical framework has been established for its thermodynamic foundation), it is used in this work to simplify the mathematical model. In practice, this assumption does not hold in all cases. Rä msch and coworkers, for instance, found that in aqueous two-phase systems containing urea, the slope of the tie-lines for PEG 3000 systems remained constant for various urea concentrations, while the slope of the tie-lines for PEG 6000 systems decreased with increasing urea concentration [10].

The equations of the tie-lines are given by:

$$C_{\mathrm{p1,T}} = MC_{\mathrm{p2,T}} + \mathrm{INT} \tag{10}$$

and

$$C_{\mathrm{p1,B}} = MC_{\mathrm{p2,B}} + \mathrm{INT} \tag{11}$$

where M is the slope and INT is the y-intercept. Following the work of Mistry et al. [8], INT is calculated by using the composition of the inlet stream (F_{in}, in this case) such that:

$$C_{\mathrm{p1,in}} = MC_{\mathrm{p2,in}} + \mathrm{INT} \tag{12}$$

As a result, Eqs. (10) and (11) become:

$$C_{\mathrm{p1,T}} = MC_{\mathrm{p2,T}} + C_{\mathrm{p1,in}} - MC_{\mathrm{p2,in}} \tag{13}$$

and

$$C_{\mathrm{p1,B}} = MC_{\mathrm{p2,B}} + C_{\mathrm{p1,in}} - MC_{\mathrm{p2,in}} \tag{14}$$

The system is described by Eqs. (2)–(8), (13), and (14).

Because of the nonlinear terms involved, it is difficult to provide a closed-form solution of the above set of equations. Also, for a numerical solution, the model equations are not easily amenable to standard mathematical software packages, without further manipulations. In most of these computational packages, only single variable derivatives are accepted.

3. Degree of freedom analysis of single-stage ATPS

Degree of freedom (DF) analysis is important for control implementation. The number of degrees of freedom, or

Table 1
The number of process variables, disturbances and parameters (variables with preset values) for the single stage ATPS

Variables	Distubances	Preset variables
V_T		V_T
$C_{p1,T}$		
$C_{p2,T}$		
$C_{i,T}$		
F_T		F_T
V_B		V_B
$C_{p1,B}$		
$C_{p2,B}$		
$C_{i,B}$		
F_B		F_B
F_{in}	F_{in}	
$C_{p1,in}$	$C_{p1,in}$	
$C_{2,in}$	$C_{p2,in}$	
$C_{i,in}$	$C_{i,in}$	
Total: $11 + 3i$	Total: $3 + i$	Total: 4

simply the freedom (f) of a process, consists of the number of independent variables that must be specified, a priori, for a complete description and adequate control of a plant [11]. This number is defined by:

$$f = N - E \tag{15}$$

where N, and E are the number of variables and model equations, respectively. This number must be zero in order to obtain a unique solution for a defined system. A total of $11 + 3i$ variables (Table 1) and $7 + 2i$ equations (Table 2) are identified for the single-stage continuous aqueous two-phase system. The freedom of the process is then $4 + i$. Thus, $4 + i$ variables need to be specified in order to solve the model. Since the flow rate and composition of feed entering (F_{in}, $C_{i,in}$, $C_{p1,in}$, and $C_{p2,in}$) are usually defined by the unit preceding the ATPS, they are treated as disturbances (Table 1) and can be removed from Eq. (15). A one-degree of freedom system is then obtained (DF = [11 + 3i] variables − [3 + i] disturbances − [7 + 2i] equations) for the dynamic process. To limit the scope of the study, we will assume that the volumetric holdups of both phases remain constant and that the outlet flow rate values, calculated from steady-state analysis, are pre-set by the operator (Table 1). As a result, Eq. (2) is not used throughout the rest of the paper. The final degree of freedom is −2 (DF = [11 + 3i] variables − [3 + i] disturbances − [6 + 2i] equations −4 preset variables). This is equivalent to a system of $6 + 2i$ equations in $4 + i$ unknowns. For the steady-state case, the volumes of the top and bottom phases are not included in the model equations; therefore the freedom of the system is −1 (DF = [9 + 3i] variables − [3 + i] disturbances − [7 + 2i] equations). This is equivalent to a system of $7 + 2i$ equations in $6 + i$ unknowns. An exact solution does not exist for these problems. In this case, it is convenient to minimize the sum of squares of $7 + 2i$ equations of $6 + i$ variables. A solution, that approximately satisfies all the equations, can then be obtained. These issues routinely arise in complex engineering problems. Parameter estimation problems, for instance, inevitably lead to an overdetermined system, since they consist of more equations than unknowns.

Table 2
The number of equations for the single stage ATPS

Model equations (eq. #)	Number of equations
Continuity equation (2)	1
Component balance (3–5)	$i + 2$
Partition coefficient (6)	i
Binodal curve-top layer (7)	1
Binodal curve-bottom layer (8)	1
Tie-line equations (13, 14)	2
Total	$7 + 2i$

4. Protein extraction using steady-state ATPS analysis

Based on the control objective, process engineers attempt to identify favorable operating conditions of a plant under the most advantageous process constraints. The computed values are typically implemented via controllers to keep the process as close as possible to setpoints. This procedure usually involves numerical optimization techniques based on steady-state analyses of a given plant. Consequently, it is important to calculate steady-state solutions of ATPS for protein extraction to maximize process performance.

The steady-state solution of the process, considered in this study, is obtained by using Eqs. (6)–(8), (13) and (14) and setting the left-hand side of Eqs. (2)–(5) to zero:

$$F_{in} - F_T - F_B = 0 \tag{16}$$

$$F_{in}C_{i,in} - F_TC_{i,T} - F_BC_{i,B} = 0 \tag{17}$$

$$F_{in}C_{p1,in} - F_TC_{p1,T} - F_BC_{p1,B} = 0 \tag{18}$$

$$F_{in}C_{p2,in} - F_TC_{p2,T} - F_BC_{p2,B} = 0 \tag{19}$$

Since the above equations represent an overspecified set of equations (degree of freedom = −1), an exact solution is unlikely. A numerical search technique, based on a least squares approach, is proposed to minimize the squared error [12]. The procedure takes advantage of the fact that the solution Z for a system $g(Z) = 0$ with $g(Z) = [g_1(Z), g_2(Z), \ldots, g_n(Z)]$ is equivalent to the minimum of the function $\zeta = g_1^2(Z) + g_2^2(Z) + g_n^2(Z)$. When there is an overspecified set of equations, redundant information is usually discarded, before a unique solution is obtained. This is not the case in the model considered in this study. In fact, a closer inspection of the two-stage system, developed by Mistry et al. [8], revealed a system of 30 equations in 28 unknowns.

5. Protein extraction using transient ATPS analysis

Although key parameters affecting pertinent process outputs can be identified from a steady-state analysis [13], time

domain information is lacking. As a result, it is very difficult to implement a procedure to accelerate process startup. Also, because of continuous fluctuations in feed flow rates and compositions of chemical processes, steady-state operations are difficult to achieve [14]. Thus, an understanding of process dynamics is a prerequisite to efficient process control.

Except for a few contributions, such as the work of Minstry and co-workers who proposed a steady-state model of continuous ATPS [8,15], modeling effort has been devoted to understanding contributing factors to protein partitioning [16]. These studies are indispensable and aid in large-scale operation. However, for control purposes, a branch dealing with modeling and simulation of transient behavior using the results of these studies is also important. A numerical scheme, based on Euler's method, is proposed to describe the process variables as they evolve from startup to equilibrium.

To study ATPS dynamic behavior, consider an application, in which, the compositions of individual components in the mixture are slightly deviated from their steady-state values ($C_{i,\mathrm{Ts}}$, $C_{i,\mathrm{Bs}}$, $C_{\mathrm{p1,Ts}}$, $C_{\mathrm{p1,Bs}}$, $C_{\mathrm{p2,Ts}}$, $C_{\mathrm{p2,Bs}}$). For the sake of simplicity, the inlet and outlet flow rates (F_{in}, F_{T}, F_{B}) remain unchanged. It is important that the deviations in compositions be small enough to have negligible influence on the system parameters. It is possible that the system has deviated from its normal operating conditions as a result of a small and short-lived perturbation in the inlet stream compositions. We are interested in computing the dynamic profile as the process settles back to its steady-state solution. For this problem, the new set of initial conditions is: $C_{i,\mathrm{T0}}$, $C_{i,\mathrm{B0}}$, $C_{\mathrm{p1,T0}}$, $C_{\mathrm{p1,B0}}$, $C_{\mathrm{p2,T0}}$, $C_{\mathrm{p2,B0}}$. The dynamic profiles resulting from these step changes can be calculated as follows:

- Step 1: Definition of initial conditions: $C_{i,\mathrm{T0}}$, $C_{i,\mathrm{B0}}$, $C_{\mathrm{p1,T0}}$, $C_{\mathrm{p1,B0}}$, $C_{\mathrm{p2,T0}}$, $C_{\mathrm{p2,B0}}$.
- Step 2: Iteration at the first sampling time ($k = 1$) using Eqs. (3)–(5) gives:

$$h_{k=\mathbf{1}} = \begin{bmatrix} F_{\mathrm{in}}C_{i,\mathrm{in}} - F_{\mathrm{T}}C_{i,\mathrm{T}} - F_{\mathrm{B}}C_{i,\mathrm{B}} \\ F_{\mathrm{in}}C_{\mathrm{p1,in}} - F_{\mathrm{T}}C_{\mathrm{p1,T}} - F_{\mathrm{B}}C_{\mathrm{p1,B}} \\ F_{\mathrm{in}}C_{\mathrm{p2,in}} - F_{\mathrm{T}}C_{\mathrm{p2,T}} - F_{\mathrm{B}}C_{\mathrm{p2,B}} \end{bmatrix}_{k=1} \tag{20}$$

Eq. (20) is obtained by setting the right-hand side of Eqs. (3)–(5) to $h_{\boldsymbol{k=1}}$. Using the initial conditions, Eq. (20) can be rewritten as:

$$h_{k=1} = \begin{bmatrix} F_{\mathrm{in}}C_{i,\mathrm{in}} - F_{\mathrm{T}}C_{i,\mathrm{T0}} - F_{\mathrm{B}}C_{i,\mathrm{B0}} \\ F_{\mathrm{in}}C_{\mathrm{p1,in}} - F_{\mathrm{T}}C_{\mathrm{p1,T0}} - F_{\mathrm{B}}C_{\mathrm{p1,B0}} \\ F_{\mathrm{in}}C_{\mathrm{p2,in}} - F_{\mathrm{T}}C_{\mathrm{p2,T0}} - F_{\mathrm{B}}C_{\mathrm{p2,B0}} \end{bmatrix}_{k=1} \tag{21}$$

After applying of a basic forward Euler computation scheme to approximate the time derivatives of Eqs. (3)–(5), the following expressions are obtained:

$$\begin{aligned} s_{k=1}[i] &= [V_{\mathrm{T}}C_{i,\mathrm{T}} + V_{\mathrm{B}}C_{i,\mathrm{B}}]_{k=1} \\ &= h_{k=1}[i]\,\Delta t + V_{\mathrm{T}}C_{i,\mathrm{T0}} + V_{\mathrm{B}}C_{i,\mathrm{B0}} \end{aligned} \tag{22}$$

$$\begin{aligned} s_{k=1}[n+1] &= [V_{\mathrm{T}}C_{\mathrm{p1,T}} + V_{\mathrm{B}}C_{\mathrm{p1,B}}]_{k=1} \\ &= h_{k=1}[n+1]\,\Delta t + V_{\mathrm{T}}C_{\mathrm{p1,T0}} + V_{\mathrm{B}}C_{\mathrm{p1,B0}} \end{aligned} \tag{23}$$

$$\begin{aligned} s_{k=1}[n+2] &= [V_{\mathrm{T}}C_{\mathrm{p2,T}} + V_{\mathrm{B}}C_{\mathrm{p2,B}}]_{k=1} \\ &= h_{k=1}[n+2]\,\Delta t + V_{\mathrm{T}}C_{\mathrm{p2,T0}} + V_{\mathrm{B}}C_{\mathrm{p2,B0}} \end{aligned} \tag{24}$$

with $i = 1{:}n$ and n is the total number of biomolecules and the other components in the system (p_1 and p_2 are not included). The variable $h_{\boldsymbol{k=1}}$ in Eq. (21) is substituted into Eqs. (22)–(24) by using:

$$h_{k=1} = [h_{k=1}[i],\ h_{k=1}[n+1],\ h_{k=1}[n+2]] \tag{25}$$

Both $h_{k=1}[i]$ and $s_{k=1}[i]$are vectors of length n.

The following relations hold:

$$K_i = \left[\frac{C_{i,\mathrm{T}}}{C_{i,\mathrm{B}}}\right]_{k=1} \tag{26}$$

$$[C_{\mathrm{p1,T}} = f_a(C_{\mathrm{p2,T}})]_{k=1} \tag{27}$$

$$[C_{\mathrm{p1,B}} = f_{\mathrm{a}}(C_{\mathrm{p2,B}})]_{k=1} \tag{28}$$

$$[C_{\mathrm{p1,T}} = MC_{\mathrm{p2,T}} + C_{\mathrm{p1,in}} - MC_{\mathrm{p2,in}}]_{k=1} \tag{29}$$

and

$$[C_{\mathrm{p1,B}} = MC_{\mathrm{p2,B}} + C_{\mathrm{p1,in}} - MC_{\mathrm{p2,in}}]_{k=1} \tag{30}$$

To solve the set of Eqs. (22)–(24), (26)–(30) ($6 + 2i$ equations) in $4 + 2i$ unknown variables ($C_{i,\mathrm{T}}$, $C_{i,\mathrm{B}}$, $C_{\mathrm{p1,T}}$, $C_{\mathrm{p1,B}}$, $C_{\mathrm{p2,T}}$, $C_{\mathrm{p2,B}}$), the system is written as a minimization problem of the form:

$$\min_{[C_{i,\mathrm{T}},\, C_{i,\mathrm{B}},\, C_{\mathrm{p1,T}},\, C_{\mathrm{p_{1,B}}},\, C_{\mathrm{p_{2,T}}},\, C_{\mathrm{p_{2,B}}}]_{k=1}}(G) \tag{31}$$

with

$$\begin{aligned} G = &\sum_{i=1}^{N}([V_{\mathrm{T}}C_{i,\mathrm{T}} + V_{\mathrm{B}}C_{i,\mathrm{B}}]_{k=1} - s_{k=1}[i])^2 \\ &+ ([V_{\mathrm{T}}C_{\mathrm{p1,T}} + V_{\mathrm{B}}C_{\mathrm{p1,B}}]_{k=1} - s_{k=1}[n+1])^2 \\ &+ ([V_{\mathrm{T}}C_{\mathrm{p2,T}} + V_{\mathrm{B}}C_{\mathrm{p2,B}}]_{k=1} - s_{k=1}[n+2])^2 \\ &+ \sum_{i=1}^{N}([K_iC_{i,\mathrm{B}} - C_{i,\mathrm{T}}]_{k=1})^2 \\ &+ ([C_{\mathrm{p1,T}} - f_{\mathrm{a}}(C_{\mathrm{p2,T}})]_{k=1})^2 \\ &+ ([C_{\mathrm{p1,B}} - f_{\mathrm{a}}(C_{\mathrm{p2,B}})]_{k=1})^2 \\ &+ ([C_{\mathrm{p1,T}} - (MC_{\mathrm{p2,T}} + C_{\mathrm{p1,in}} - MC_{\mathrm{p2,in}})]_{k=1})^2 \\ &+ ([C_{\mathrm{p1,B}} - (MC_{\mathrm{p2,B}} + C_{\mathrm{p1,in}} - MC_{\mathrm{p2,in}})]_{k=1})^2 \end{aligned} \tag{32}$$

- Step 3: repeat the above procedure for $k + 1$.
- Step 4: stop at the end of the simulation.

6. Results

6.1. Steady-state continuous ATPS

The case study is adapted from the work of Minstry at al. [8]and experimental data from Cascone et al. [17]. The original process was aimed at separating thaumatin from *Escherichia coli* contaminants with the addition of sodium chloride to the system. The components were thaumatin, NaCl, and contaminant proteins with two phases formed by PEG and phosphate salt. The process included two purification stages and a recycle stream (Fig. 3). The bulk of the separation took place in STAGE 1 with the product moving to the top phase (PEG-rich phase). STAGE 2 was used to partition the product back to the bottom phase (Phosphate-rich phase). The top phase was, then, recycled. These two stages consisted of six different streams, including a waste outlet stream from the first stage and a recycle stream. The flow rate connecting the two stages and the compositions of the streams were the process variables. The steady-state model was solved (Fig. 3), in this research, using a constrained minimization function "fmincon" from the Matlab Optimization Toolbox (MathWorks, Inc.). Only the underlined values were given in the original work. The results shown in Fig. 3 form the basis for the simulation work presented in this paper.

STAGE 1 of Fig. 3 is used in this simulation to study a single-stage continuous aqueous two-phase system (similar to Fig. 1). The two inlet streams (F_1 and F_2), in the original study, are combined into a single stream (F_{in}). The various flow rates and component concentrations are calculated using the relations:

$$C_{j,\mathrm{in}} = \frac{F_1 C_{j,1} + F_2 C_{j,2}}{F_1 + F_2}; \quad C_{j,\mathrm{T}} = C_{j,4};\ C_{j,\mathrm{B}} = C_{j,3};$$
$$F_{\mathrm{T}} = F_4;\ F_{\mathrm{B}} = F_3;\ F_{\mathrm{in}} = F_1 + F_2 \tag{33}$$

where $C_{j,\mathrm{in}}$, $C_{j,\mathrm{T}}$, $C_{j,\mathrm{B}}$, F_{T}, F_{B}, F_{in} are the inlet, top and bottom stream concentrations and flow rates, respectively (Fig. 1). The subscript j represents the components, including p_1 and p_2. The single-stage unit consists of five components: sodium salt NaCl (C_{SALT}), contaminant (C_{CON}), desired protein (C_{PRO}), polyethylene (glycol) (C_{PEG}), and phosphate salt (C_{PSAL}). The inlet stream composition and flow rate are listed in Table 3. The inlet flow rate was then increased by 50% (from $F_{\mathrm{in}} = 13.03$ to $19.54\,\mathrm{m^3\,s^{-1}}$) to further verify the numerical procedure. An increase in the flow rate should not affect the concentrations of the outlet stream. After recasting the system as a minimization problem (Eq. (31)), a constrained optimization procedure, "fmincon", from the Matlab Optimization Toolbox (MathWorks, Inc.), was used to solve the problem. The results are shown in the last two columns of Table 3. The variables were constrained to values between 0.00 and 200.0. As expected, only the top and bottom flow rate values change. A comparison (using $F_{\mathrm{in}} = 13.03\,\mathrm{m^3\,s^{-1}}$) with the values, reported in Fig. 3, shows good agreement (Flow streams F_{B} and F_{T} in Fig. 1 correspond to streams F_3 and F_4, respectively, in Fig. 3).

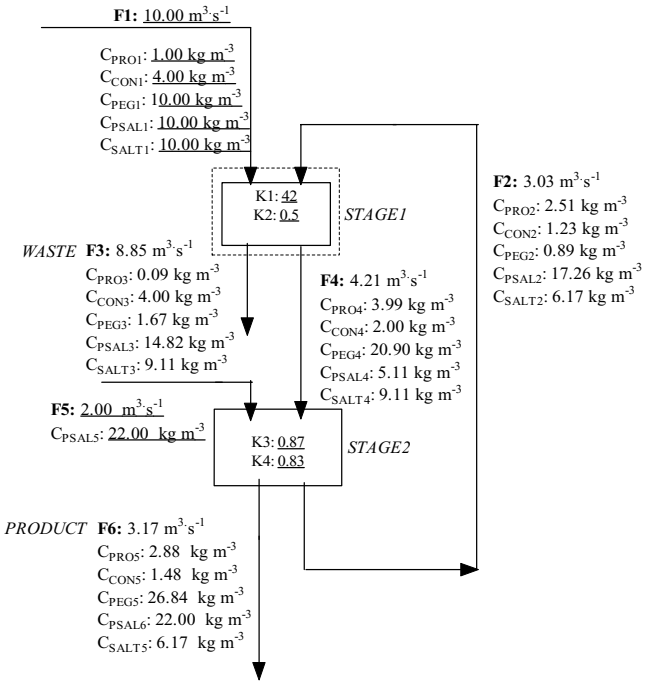

Fig. 3. Flow scheme of the aqueous two-phase continuous protein extraction. The flow rates and concentrations were obtained after solving the system given in Mistry et al. [8]. Only the underlined values were given in the original work.

Table 3
Solutions for the steady state continuous ATPS problem

Variables	Known variables	Numerical values	Solution*	Solution**
$C_{\mathrm{PEG,T}}$			20.91	20.90
$C_{\mathrm{PSAL,T}}$			5.11	5.11
$C_{\mathrm{PRO,T}}$			3.99	3.99
$C_{\mathrm{CON,T}}$			2.00	2.00
$C_{\mathrm{SALT,T}}$			9.16	9.11
F_{T}			4.20	6.31
$C_{\mathrm{PEG,B}}$			1.69	1.67
$C_{\mathrm{PSAL,B}}$			14.82	14.82
$C_{\mathrm{PRO,B}}$			0.10	0.09
$C_{\mathrm{CON,B}}$	‘		4.00	4.00
$C_{\mathrm{SALT,B}}$			9.09	9.11
F_{B}			8.83	13.24
$C_{\mathrm{PEG,in}}$	$C_{\mathrm{PEG,in}}$	7.88		
$C_{\mathrm{PSAL,in}}$	$C_{\mathrm{PSAL,in}}$	11.69		
$C_{\mathrm{PRO,in}}$	$C_{\mathrm{PRO,in}}$	1.35		
$C_{\mathrm{CON,in}}$	$C_{\mathrm{CON,in}}$	3.35		
$C_{\mathrm{SALT,in}}$	$C_{\mathrm{SALT,in}}$	9.11		
F_{in}	F_{in}	13.03*; 19.54**		

The inlet stream composition and flow rate are listed. Solution* and solution** correspond to inlet flow rate of 13.03 and $19.54\,\mathrm{m^3\,s^{-1}}$, respectively.

Table 4
Concentration values after 2.08 h

Variables	Known variables	Operating condition	Initial values	SS solution* ($t = 2.08$ h)	SS solution** ($t = 2.08$ h)
V_T	V_T	13188.09			
$C_{PEG,T}$			16.73	19.26	19.98
$C_{PSAL,T}$			4.09	5.57	5.36
$C_{PRO,T}$			3.19	3.92	3.96
$C_{CON,T}$			1.60	1.99	2.06
$C_{SALT,T}$			7.33	9.14	9.16
F_T		4.20*; 6.31*			
V_B	V_B	3338.89			
$C_{PEG,B}$			1.35	2.05	1.92
$C_{PSAL,B}$			11.86	14.66	14.72
$C_{PRO,B}$			0.08	0.09	0.09
$C_{CON,B}$			3.20	3.90	4.09
$C_{SALT,B}$			7.27	9.06	9.04
F_B		8.83*; 13.24*			
$C_{PEG,in}$	$C_{PEG,in}$	7.88			
$C_{PSAL,in}$	$C_{PSAL,in}$	11.69			
$C_{PRO,in}$	$C_{PRO,in}$	1.35			
$C_{CON,in}$	$C_{CON,in}$	3.35			
$C_{SALT,in}$	$C_{SALT,in}$	9.11			
F_{in}	F_{in}	13.03*; 19.54**			

This time length was chosen to make sure that the system has reached steady-state. The flow rates used to study the dynamic behavior of the system were the values obtained in the steady state case (Table 3). $F_T = 4.20$, $F_B = 8.83$, $F_{in} = 13.03\,m^3\,s^{-1}$in one case, and $F_T = 6.31$, $F_B = 13.24$, $F_{in} = 19.54\,m^3\,s^{-1}$ in another case.

6.2. Unsteady-state continuous ATPS

Following the pilot scale enzyme purification of Boland et al. [18] using ATPS, dilution rates of 3.19×10^{-4} and $1.26 \times 10^{-3}\,s^{-1}$ were used for the top and bottom layers, respectively. Consequently, the volumes of the top and bottom layers are $V_T = 13{,}188.09$ and $V_B = 3338.89\,m^3$. The flow rates were fixed (F_{in}, F_T, F_B) at their steady-state values. A step change decrease of 20% in top and bottom phase concentrations was applied to the system in order to provide initial conditions for the simulation. For the purpose of the study, the unit operated continuously for 2.1 h. As in the steady-state case, two different feed flow rates were chosen: $F_{in} = 13.03$ and $19.54\,m^3\,s^{-1}$. The results of the simulation are shown in Figs. 4–13. The concentrations at the end of the simulation are listed in Table 4 for both flow rates. For $F_{in} = 13.03\,m^3\,s^{-1}$, the following observations were made (Figs. 4–8): after the perturbation, the components of the system exhibited different dynamical behaviors in reaching their steady-state concentrations values; in accordance with a partition coefficient of 0.5, the concentration of undesired protein was higher in the bottom layer than in the top layer (Fig. 7); sodium chloride concentration profiles in the top and bottom phases were similar (Fig. 8), consistent with a partition coefficient of 1; as expected, the top phase was rich in PEG (Fig. 4) while the bottom phase was rich in phosphate salt (Fig. 5). The steady-states values for the concentrations (Table 4, SS sol*) agreed, fairly well, with the values obtained in the static analysis (Table 3, solution*). Similar trends and ultimate concentration values were obtained when the inlet flow rate was increased by 50% ($F_{in} = 19.54\,m^3\,s^{-1}$) (compare Table 4, SS sol** with Table 3, solution**). These results show the efficiency of the method in predicting the process transient behavior. The noise could be reduced greatly by using a smaller step size. However, this may introduce considerable computational overhead. A step size of 1 s was used in the study.

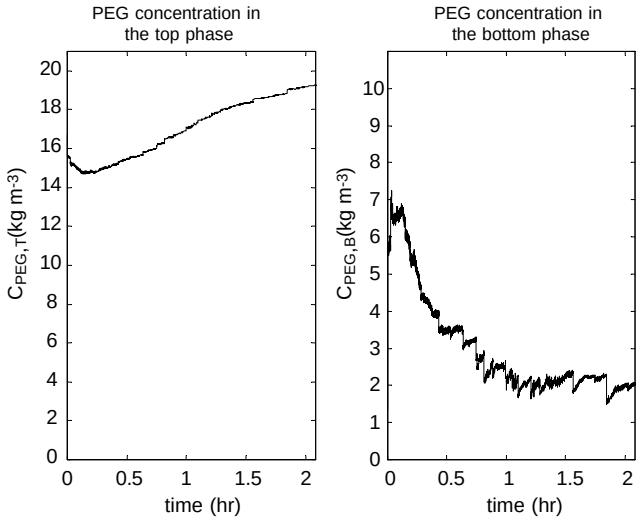

Fig. 4. Concentrations profiles of PEG in the top ($C_{PEG,T}$) and bottom phases ($C_{PEG,B}$). A step change decrease of 20% in top and bottom phase concentrations was applied to the system in order to provide initial conditions for the simulation. The inlet flow rate was set to $F_{in} = 13.03\,m^3\,s^{-1}$.

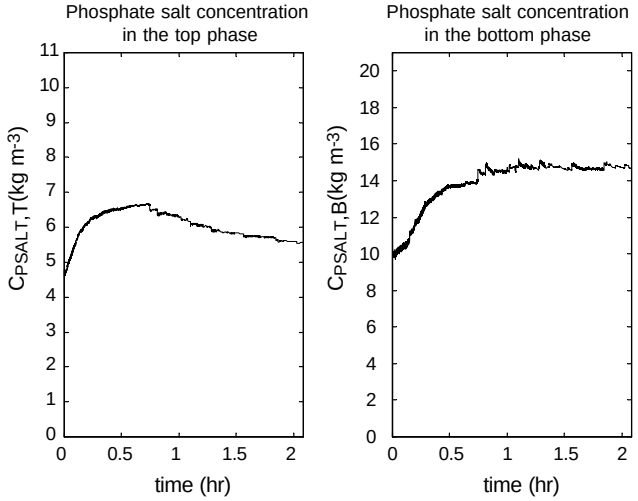

Fig. 5. Concentrations profiles of phosphate salt in the top ($C_{PSAL,T}$) and bottom phases ($C_{PSAL,B}$). A step change decrease of 20% in top and bottom phase concentrations was applied to the system in order to provide initial conditions for the simulation. The inlet flow rate was set to $F_{in} = 13.03\,m^3\,s^{-1}$.

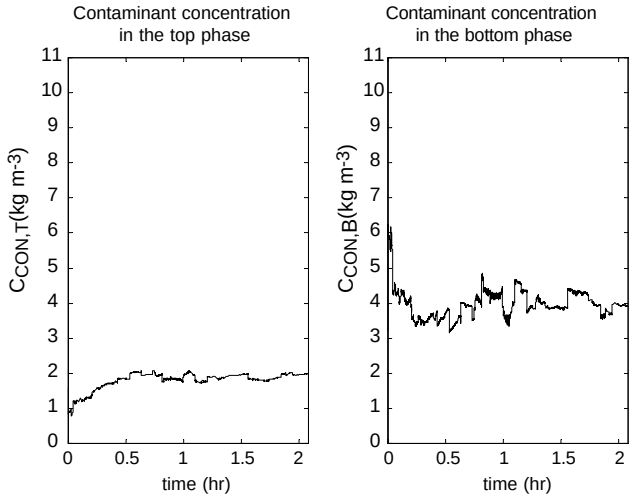

Fig. 7. Concentrations profiles of contaminants in the top ($C_{CON,T}$) and bottom phases ($C_{CON,B}$). A step change decrease of 20% in top and bottom phase concentrations was applied to the system in order to provide initial conditions for the simulation. The inlet flow rate was set to $F_{in} = 13.03\,m^3\,s^{-1}$.

6.3. Input–output continuous ATPS model

In process control applications, it is customary to perform open-loop analysis in order to determine possible control strategies. Such input–output models allow the process engineer to investigate the response of pertinent process variables to changes in the input variables. Section 6.1 outlines a steady-state analysis to compute equilibrium values of ATPS state variables and flow rates. Section 6.2 shows how the interested variables reach their setpoint values. From Figs. 5 and 8, for instance, it is evident that state variables, such as sodium chloride (C_{SALT}) and phosphate salt (C_{PSAL}) concentrations, settle to their final values at different times. These observations cannot be based on steady-state analysis alone.

This section investigates how the output variables ($C_{SALT,T}$, $C_{SALT,B}$, $C_{CON,T}$, $C_{CON,B}$, $C_{PRO,B}$, $C_{PRO,T}$, $C_{PEG,T}$, $C_{PEG,B}$, $C_{PSAL,T}$, $C_{PSAL,B}$) respond to a 4% step change decrease in the inlet stream flow rate ($F_{in} = 13.03$–$12.51\,m^3\,s^{-1}$) and component concentrations. The initial conditions used in the simulation for the transient case correspond to the steady-state solution prior to the step change (Table 3: solution*). The Euler's method was, again, implemented to solve the set of equations. At high

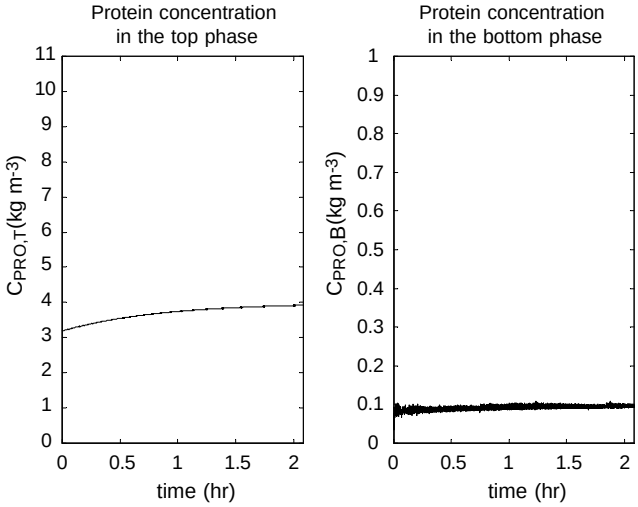

Fig. 6. Concentrations profiles of target protein in the top ($C_{PRO,T}$) and bottom phases ($C_{PRO,B}$). A step change decrease of 20% in top and bottom phase concentrations was applied to the system in order to provide initial conditions for the simulation. The inlet flow rate was set to $F_{in} = 13.03\,m^3\,s^{-1}$.

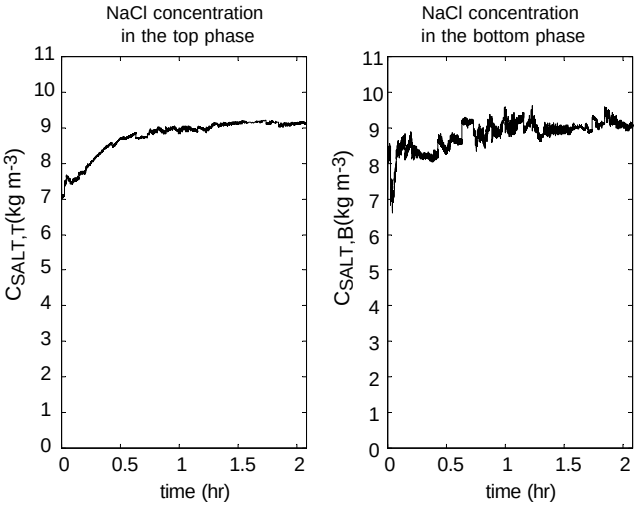

Fig. 8. Concentrations profiles of sodium salt in the top ($C_{SALT,T}$) and bottom phases ($C_{SALT,B}$). A step change decrease of 20% in top and bottom phase concentrations was applied to the system in order to provide initial conditions for the simulation. The inlet flow rate was set to $F_{in} = 13.03\,m^3\,s^{-1}$.

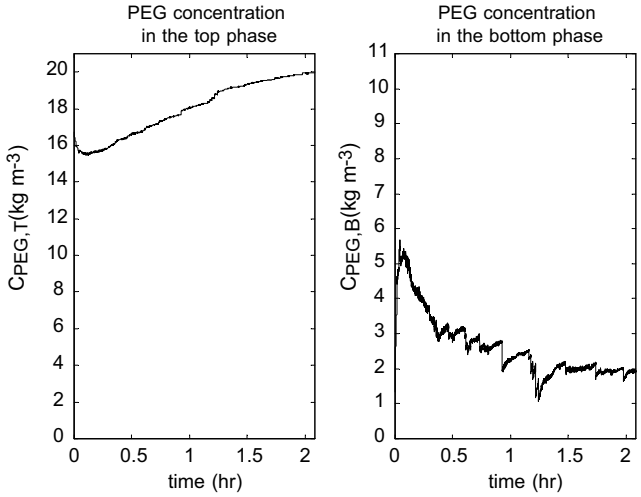

Fig. 9. Concentrations profiles of PEG in the top ($C_{PEG,T}$) and bottom phases ($C_{PEG,B}$). A step change decrease of 20% in top and bottom phase concentrations was applied to the system in order to provide initial conditions for the simulation. The inlet flow rate was set to $F_{in} = 19.54\,m^3\,s^{-1}$.

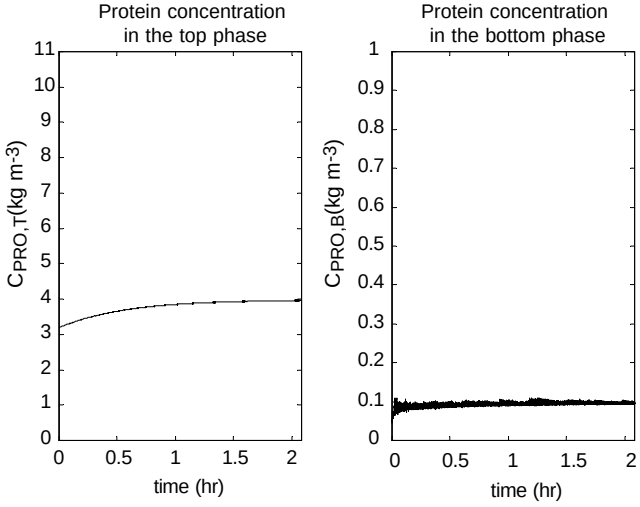

Fig. 11. Concentrations profiles of target protein in the top ($C_{PRO,T}$) and bottom phases ($C_{PRO,B}$). A step change decrease of 20% in top and bottom phase concentrations was applied to the system in order to provide initial conditions for the simulation. The inlet flow rate was set to $F_{in} = 19.54\,m^3\,s^{-1}$.

disturbance, the algorithm tends to diverge, as indicated by a large value for the sum of square errors. Steady-state and transient behaviors were studied and the results are shown in Tables 5 and 6 and Figs. 14–18. The simulation was allowed to run for a longer period (2.78 h) to allow the system to settle to its new steady state after initiating the perturbation. A comparison of the concentrations at the end of the simulation (Table 6, SS sol. ($t = 2.78$ h)) with those from the steady-state analysis (Table 5, solution) revealed similar results. In the context of process control, open-loop response tests are crucial. These tests allow the control engineer to determine the process time constant, gain and deadtime. Using these parameters, classical PID controller tuning methods can be implemented resulting in improved loop performance. The overall benefit is a better control of the process and increased productivity.

7. Effects of the density difference between the two phases

Phase separations occur by centrifugation with the density difference as the driving force. Although both phases in aqueous two-phase systems contain mainly water, it is useful to investigate the effect of the difference in phase

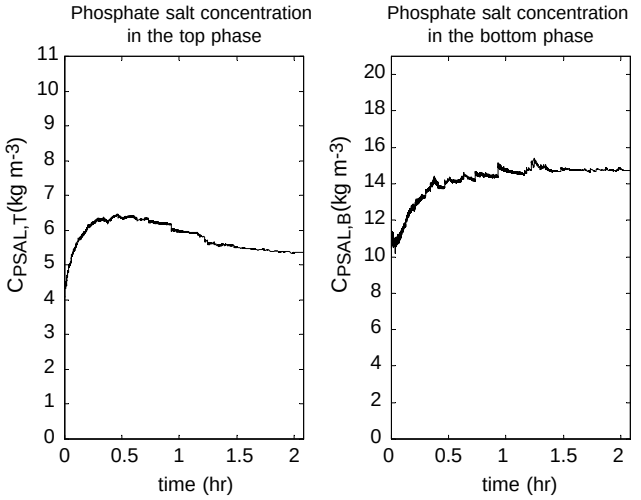

Fig. 10. Concentrations profiles of phosphate salt in the top ($C_{PSAL,T}$) and bottom phases ($C_{PSAL,B}$). A step change decrease of 20% in top and bottom phase concentrations was applied to the system in order to provide initial conditions for the simulation. The inlet flow rate was set to $F_{in} = 19.54\,m^3\,s^{-1}$.

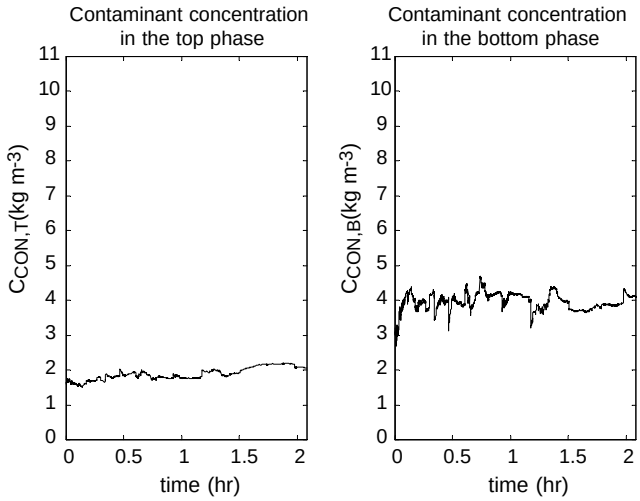

Fig. 12. Concentrations profiles of contaminants in the top ($C_{CON,T}$) and bottom phases ($C_{CON,B}$). A step change decrease of 20% in top and bottom phase concentrations was applied to the system in order to provide initial conditions for the simulation. The inlet flow rate was set to $F_{in} = 19.54\,m^3\,s^{-1}$.

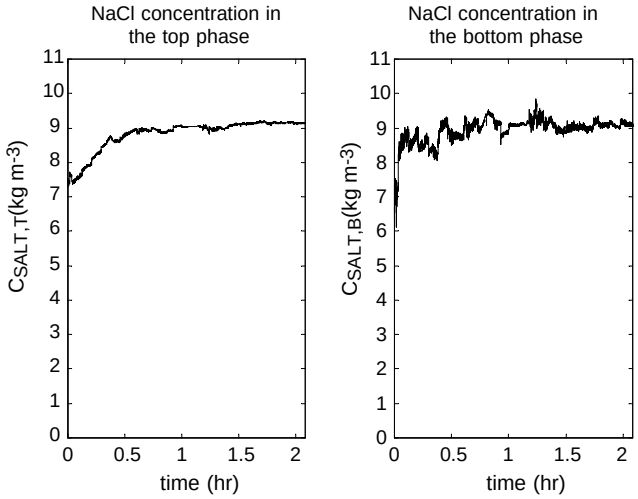

Fig. 13. Concentrations profiles of sodium salt in the top ($C_{SALT,T}$) and bottom phases ($C_{SALT,B}$). A step change decrease of 20% in top and bottom phase concentrations was applied to the system in order to provide initial conditions for the simulation. The inlet flow rate was set to $F_{in} = 19.54\,m^3\,s^{-1}$.

densities on the ultimate concentrations of the system. The main difference with the above analysis is that Eq. (1) is now replaced by:

$$\rho_{in}F_{in} - \rho_T F_T - \rho_B F_B = 0 \quad (34)$$

For the purpose of the study, the density of the inlet flow (heterogeneous mixture) is taken as the average of the densities of the top and bottom phase. We will consider two particular cases. A) One in which the density difference of the two phases is $100\,kg/m^3$. B) The other in which the density difference of the two phases is $40\,kg/m^3$. An average density of $\rho_T = 1077\,kg/m^3$ is used for the top phase. As a result $\rho_B = 1177\,kg/m^3$ and $\rho_{in} = 1127\,kg/m^3$ for case A and $\rho_B = 1117\,kg/m^3$ and $\rho_{in} = 1097\,kg/m^3$ for case B. The algorithm is designed to minimize a weighted mean square error function so that the individual functions $g_1(Z)$, $g_2(Z)$, ..., $g_n(Z)$ (see Section 5) are of the same order of magnitude. The results are listed in Table 7. Columns solution A and solution B show that there was no significant difference between the two cases.

Table 5
Solution for the steady continuous ATPS problem obtained by decreasing the original inlet stream flow rate and component composition (Table 3, numerical values, $F_{in} = 13.03\,m^3\,s^{-1}$) by 4%

Variables	Known variables	Numerical values	Solution
$C_{PEG,T}$			18.88
$C_{PSAL,T}$			5.50
$C_{PRO,T}$			3.79
$C_{CON,T}$			1.92
$C_{SALT,T}$			8.74
F_T			4.08
$C_{PEG,B}$			2.08
$C_{PSAL,B}$			13.99
$C_{PRO,B}$			0.09
$C_{CON,B}$			3.85
$C_{SALT,B}$			8.75
F_B			8.43
$C_{PEG,in}$	$C_{PEG,in}$	6.30	
$C_{PSAL,in}$	$C_{PSAL,in}$	9.35	
$C_{PRO,in}$	$C_{PRO,in}$	1.08	
$C_{CON,in}$	$C_{CON,in}$	2.68	
$C_{SALT,in}$	$C_{SALT,in}$	7.29	
F_{in}	F_{in}	12.51	

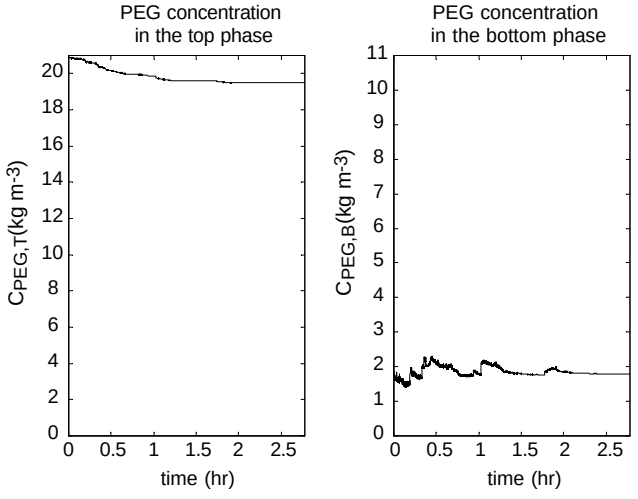

Fig. 14. Concentrations profiles of PEG in the top ($C_{PEG,T}$) and bottom phases ($C_{PEG,B}$). A step change decrease of 4% was applied in the inlet stream flow rate ($F_{in} = 13.03$–$12.51\,m^3\,s^{-1}$) and component concentrations.

8. Discussions

Although steady-state analysis provides prediction of operating conditions (Section 6.1), the response time could not

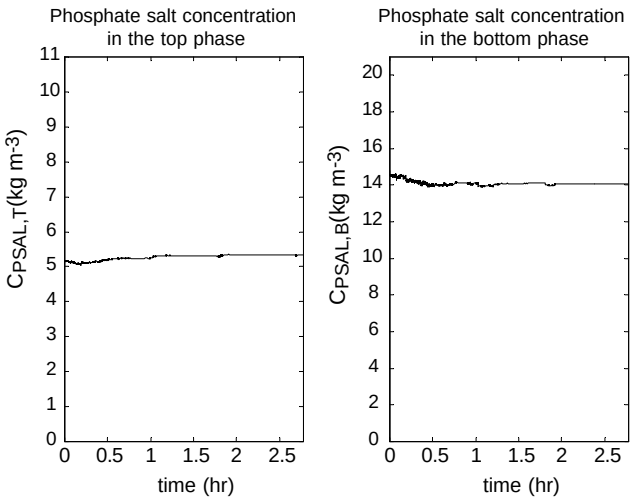

Fig. 15. Concentrations profiles of phosphate salt in the top ($C_{PSAL,T}$) and bottom phases ($C_{PSAL,B}$). A step change decrease of 4% was applied in the inlet stream flow rate ($F_{in} = 13.03$–$12.51\,m^3\,s^{-1}$) and component concentrations.

Table 6
Concentration values after 2.78 h

Variables	Known variables	Operating condition	Initial values	SS solution ($t = 2.78$ h)
V_T	V_T	13188.09		
$C_{PEG,T}$			20.91	19.47
$C_{PSAL,T}$			5.11	5.32
$C_{PRO,T}$			3.99	3.80
$C_{CON,T}$			2.00	1.91
$C_{SALT,T}$			9.16	8.65
F_T		4.08		
V_B	V_B	3338.89		
$C_{PEG,B}$			1.69	1.80
$C_{PSAL,B}$			14.82	14.08
$C_{PRO,B}$			0.10	0.09
$C_{CON,B}$			4.00	3.86
$C_{SALT,B}$			9.09	8.80
F_B		8.43		
$C_{PEG,in}$	$C_{PEG,in}$	6.30		
$C_{PSAL,in}$	$C_{PSAL,in}$	9.35		
$C_{PRO,in}$	$C_{PRO,in}$	1.08		
$C_{CON,in}$	$C_{CON,in}$	2.68		
$C_{SALT,in}$	$C_{SALT,in}$	7.29		
F_{in}	F_{in}	12.51		

This time length was chosen to make sure that the system has reached steady-state. The flow rates used to study the dynamic behavior of the system were the values obtained in the steady state case (Table 5). $F_T = 4.08$, $F_B = 8.43$, $F_{in} = 12.51\,m^3\,s^{-1}$.

be determined. Simulation of the dynamic behavior of the system allows the process engineer to estimate the response time of key process variables. The proposed methodology accurately predicts steady- and unsteady-state behaviors. It may be extended to many applications dealing with protein separations. Even though most continuous solvent extractions are carried out on a steady-state basis, possible safety and environmental risks at the earliest possible design stage need to be investigated [7]. These issues can only be addressed with a firm knowledge of the transient behavior of the process.

The benefits of continuous aqueous two-phase extractions for the purification of enzymes and other biomaterials are tremendous [19,20]. A mixer–settler extractor was used by Castro et al. [21]to separate lanthanum from a rare earth chloride mixture; a high purity of lanthanum product was obtained with a 20-stage process. Bim and Franco [22] designed a pulse caps column for the continuous extraction of alkaline xylanase. With a single-step operation, a purification factor of 33 and a yield of 98% enzyme were achieved. These works, however, did not take into account the dynamic behavior of the process. An assessment of safety and

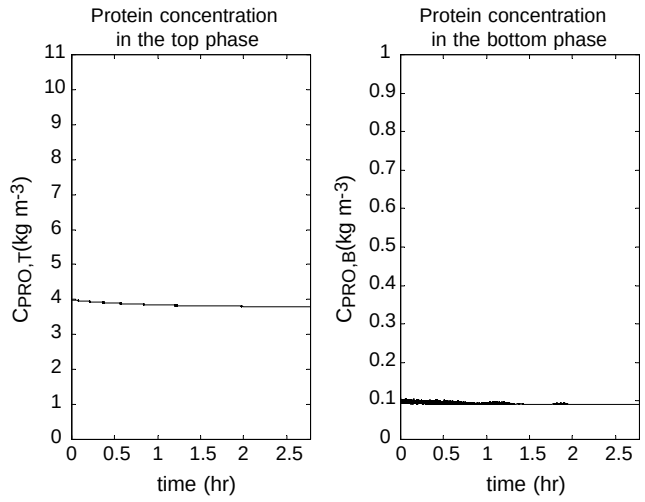

Fig. 16. Concentrations profiles of target protein in the top ($C_{PRO,T}$) and bottom phases ($C_{PRO,B}$). A step change decrease of 4% was applied in the inlet stream flow rate ($F_{in} = 13.03$–$12.51\,m^3\,s^{-1}$) and component concentrations.

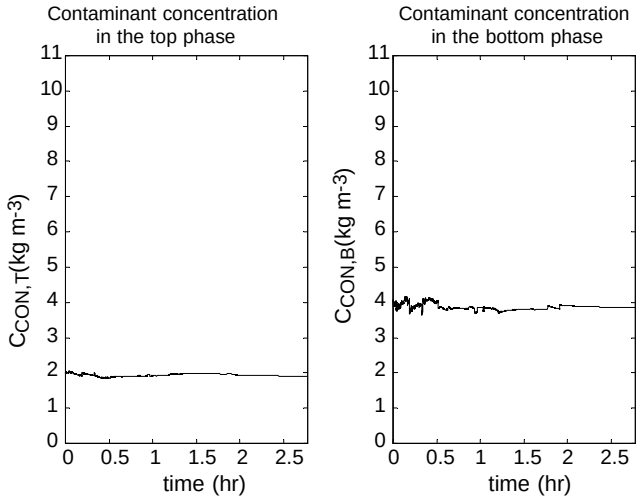

Fig. 17. Concentrations profiles of contaminants in the top ($C_{CON,T}$) and bottom phases ($C_{CON,B}$). A step change decrease of 4% was applied in the inlet stream flow rate ($F_{in} = 13.03$–$12.51\,m^3\,s^{-1}$) and component concentrations.

Table 7
Solution for the steady continuous ATPS problem using a density difference of 100 kg/m^3 (solution A) and 40 kg/m^3 (solution B) between the two phases

Variables	Known variables	Numerical values	Solution A ($\Delta\rho = 100\,kg/m^3$)	Solution B ($\Delta\rho = 40\,kg/m^3$)
$C_{PEG,T}$			21.23	21.05
$C_{PSAL,T}$			5.06	5.09
$C_{PRO,T}$			3.95	3.98
$C_{CON,T}$			2.04	2.02
$C_{SALT,T}$			9.24	9.17
F_T			4.26	4.22
$C_{PEG,B}$			1.43	1.59
$C_{PSAL,B}$			15.22	14.98
$C_{PRO,B}$			0.09	0.09
$C_{CON,B}$			4.08	4.03
$C_{SALT,B}$			9.25	9.17
F_B			8.58	8.73
$C_{PEG,in}$	$C_{PEG,in}$	7.88		
$C_{PSAL,in}$	$C_{PSAL,in}$	11.69		
$C_{PRO,in}$	$C_{PRO,in}$	1.35		
$C_{CON,in}$	$C_{CON,in}$	3.35		
$C_{SALT,in}$	$C_{SALT,in}$	9.11		
F_{in}	F_{in}	13.03		

environmental risks in the current framework would be very difficult. This paper provides a framework for transient analysis of ATPS. More advanced controllers, using model-based control methodologies (IMC and NMPC), can be used to regulate ATPS. These controllers explicitly take into account constraints and include the dynamic behavior of the plant. They would be very useful to control ATPS since these systems are nonlinear and, therefore, difficult to regulate using classical controllers. In fact, advanced control schemes have been implemented to control liquid-liquid extraction with an organic and a single aqueous phase (completely immiscible phases). Wachs et al. [23] tested an internal model controller (IMC) [24] on a Karr extraction column. Grossman and Lewin [25] also studied a Karr-type column to show the performance of a nonlinear model predictive controller (NMPC). The process dynamic model was generated using genetic programming [26], a system identification technique based on an evolutionary optimization procedure. A common feature of model-based control methodologies is the use of a mathematical model of the system transient behavior.

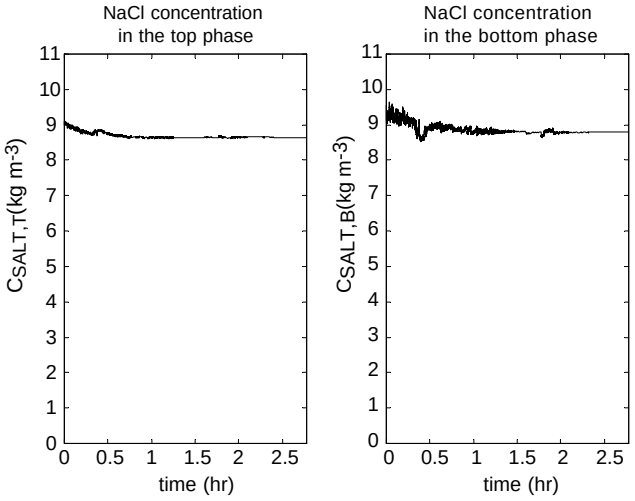

Fig. 18. Concentrations profiles of sodium salt in the top ($C_{SALT,T}$) and bottom phases ($C_{SALT,B}$). A step change decrease of 4% was applied in the inlet stream flow rate ($F_{in} = 13.03$–$12.51\,m^3\,s^{-1}$) and component concentrations.

Aqueous two-phase systems offer a unique challenge in that they are formed from solutions of partly miscible phases (two mutually incompatible polymers or a polymer and a salt), increasing the mathematical complexity of these systems, as compared to traditional liquid-liquid extraction. Since ATPS behaviors are difficult to predict, their industrial applications are limited because of a lack of mathematical models. The proposed dynamic description can be used in the context of model predictive controls to handle process non-linearity, time-varying parameters, and to meet the control objectives without constraint violation.

9. Conclusion

A mathematical model and a method of solution, based on a least squares approach, were investigated to study the static and dynamic behaviors of single-stage continuous ATPS. The methodology was tested using experimental data obtained for purification of thaumatin form *E. coli* contaminant proteins in a poly (ethylene-glycol)/phosphate salt/water system. The study was conducted assuming constant volumetric holdups of both phases. The degrees of freedom for the static and dynamic models were −2 and

−1, respectively. Results obtained for the static case agreed with published data and with ultimate concentrations values obtained in the transient case. The input–output model was simulated to instigate the responses of the components of the system to a 4% step change decrease in the inlet stream flow rate ($F_{in} = 13.03$–$12.51\,m^3\,s^{-1}$) and component concentrations. This analysis showed that the component concentrations settle to their steady-state values in different time periods. An analysis, in which the density of the inlet flow (heterogeneous mixture) was estimated as the average of the densities of the top and bottom phases, showed that the constant density assumption used to simplify the model would not introduce significant errors in the results for phase density differences as large as $100\,kg/m^3$. The proposed analysis can be used in designing a control system for continuous two-phase extraction for industrial applications.

10. Nomenclature

C	concentration of the various components
E	number of model equations
f	number of degree of freedom
F	stream flow rate
K	component partition coefficient
M	slope of the tie line
N	number of variables
V	volume

Greek letter

ρ	density

Subscripts

B	bottom layer
i	component index (not including p_1 and p_2)
in	inlet stream
p_1	top phase-rich polymer
p_2	bottom phase-rich polymer
T	top layer

References

[1] P. A. Albertsson, Partition of Cell Particles and Macromolecules, Wiley, New York, 1986.
[2] M.-R. Kula, Bioseparation 1 (1990) 181.
[3] K.S.M.S. Raghavarao, N.K. Rastogi, G.M.K. Karanth, N.G. Karanth, Adv. Appl. Microbiol. 4 (1995) 97.
[4] Q. Peng, Z.L.Y. Li, Fluid Phase Equilib. 107 (1995) 303.
[5] D.P. Petrides, A. Koulouris, P.T. Lagonikos, Pharm. Eng. 22 (2002) 56.
[6] L.H.M. Silva, A.J.A. Meirelles, Carbohyd. Polym. 42 (2000) 273.
[7] J. Ingham, I.J. Dunn, E. Heinzle, J.E. Prenosil, Chemical Engineering Dynamics: An Introduction to Modelling and Computer Simulation, Wiley-VCH, New York, 2000.
[8] S.L. Mistry, J.A. Asenjo, C.A. Zaror, Bioseparation 3 (1993) 343.
[9] H.W. Blanch, D.S. Clark, Biochemical Engineering, Marcel Dekker Inc., New York, 1997.
[10] R. ämsch, L.B. Kleinelanghorst, E.A. Knieps, J. Thömmes, M.R. Kula, Biotechnol. Progr. 15 (1999) 493.
[11] G. Stephanopoulos, Chemical Engineering Control. An Introduction to Theory and Practice, PTR Prentice Hall, Englewood Cliffs, 1984.
[12] O.T. Hanna, O.C. Sandall, Computational Methods in Chemical Engineering, Prentice Hall PTR, Upper Saddle River, NJ, 1995.
[13] T. Bibila, M. Flickinger, Biotechnol. Bioeng. 39 (1992) 251.
[14] J.B. Riggs, Chemical Process Control, second ed., Ferret Publishing, Lubbock, NJ, 2001.
[15] S.L. Mistry, A. Kaul, J.C. Merchuck, J.A. Asenjo, J. Chromatogr. A 741 (1996) 151.
[16] D. Forciniti, C.K. Hall, ACS Symp. Ser. 419 (1990) 53.
[17] O. Cascone, B.A. Andrews, J.A. Asenjo, Enzyme Microb. Technol. 13 (1991) 629.
[18] M.J. Boland, P.G.M. Hesselink, N. Papamichael, H. Hustedt, J. Biotechnol. 19 (1991) 19.
[19] H. Hustedt, K. Kroner, N. Papamichael, Process Biochem. 23 (1988) 129.
[20] L. Strandberg, K. Kohler, S.-O. Enfors, Process Biochem. 26 (1991) 225.
[21] M.G. Castro, M. Smutz, R.G. Bautista, Trans. Soc. Mining Eng. AIME 250 (1971) 42.
[22] M.A. Bim, T.T. Franco, J. Chromatogr. B 743 (2000) 349.
[23] A. Wachs, J. Benyamin, R. Semiat, D.R. Lewin, Comput. Chem. Eng. 21S (1997) S601.
[24] M. Morari, E. Zafiriou, Robust Process Control, Prentice-Hall, Englewood Cliffs, NJ, 1989.
[25] B. Grosman, D.R. Lewin, Comput. Chem. Eng. 26 (2002) 631.
[26] L. Gao, N.W. Loney, Comput. Chem. Eng. 25 (2001) 1403.